A Three-Dimensional Simulation of the Hudson–Raritan Estuary. Part III: Salt Flux Analyses

LIE-YAUW OEY* AND GEORGE L. MELLOR

Geophysical Fluid Dynamics Program, James Forrestal Campus, Princeton University, Princeton, NJ 08542

RICHARD I. HIRES

Department of Civil and Ocean Engineering, Stevens Institute of Technology, Hoboken, NJ 07030

(Manuscript received 12 December 1984, in final form 31 May 1985)

ABSTRACT

Salt fluxes and volume transports in an estuary vary considerably over subtidal time scales of a few days to weeks in response to wind and neap–spring tidal forcings. Results from a numerical simulation of the Hudson–Raritan estuary are used to study subtidal variations of salt fluxes and the physical mechanisms for salt balance in the estuary. Simulated salt fluxes are compared with available observations. Observations support the model's finding that analysis of volume and salt fluxes based on short-length data records (<30 days) can lead to misleading conclusions.

"Tidal trapping" effects due to coastline irregularities contribute most to the salt balance at the Sandy Hook–Rockaway Point transect and at the Narrows. A two-week observational record is analyzed to support this finding. Simulated subtidal variation of the tidal trapping term at the Sandy Hook–Rockaway Point transect compares well with that observed. In Raritan Bay, where tidal currents are weak and effects of winds are significant, contributions to salt balance from vertical velocity and salinity gradients are comparable to transverse contributions. This occurs despite the fact that surface-to-bottom salinity differences during the simulation period—a period of low freshwater flow–never exceed 0.5‰ throughout most regions of the bay. A two-dimensional, depth-integrated *xy–t* model, in which the horizontal dispersion coefficients are modeled empirically, may not perform well in this case.

1. Introduction

In this part of our three-part paper, we use model results obtained from a numerical simulation of the Hudson–Raritan estuary (Oey *et al.*, 1985a,b) to study various mechanisms responsible for salt transports in the estuary. Across a particular cross section in an estuary at steady state, the net salt flux is zero, which means that up-estuary advection and turbulent diffusion and/or dispersion of salt by tidal currents are balanced by down-estuary advection of salt by freshwater river discharge. In practice, subtidal forcing modifies the "steady" circulation and salt balance. Two main questions are: 1) What are the effects of subtidal forcing on various salt transport mechanisms?; and 2) What is the dominant physical mechanism responsible for up-estuary salt balance?

Because of the fine grid resolution used in our model, we can calculate, with good precision, salt fluxes across a particular section in the estuary. Observations collected by the National Ocean Survey (NOS) are also available, but these are sparsely spaced and are generally not always simultaneous in time. We have nevertheless made some salt flux calculations based on these data and have compared them with model results.

2. Salt-flux analysis

The numerical model results we shall use in the following flux analysis are from the simulation period of 22 July–26 September 1980. The amount of data is large; hence, we shall discuss only the three cross sections shown in Fig. 1: the Sandy Hook–Rockaway Point transect (henceforth the SHRP transect), the Raritan Bay and the Narrows sections.

a. Salt flux decomposition

The rate of salt transport across a section is given by

$$\dot{M} = \left\langle \int_A u_n S dA \right\rangle \tag{1}$$

where u_n is the velocity normal to the section, A is the cross-sectional area and the angle brackets denote the time average: $\langle(\cdot)\rangle = T^{-1}\int_0^T (\cdot)dt$. We follow Fischer (1972) and decompose u_n and S into their various deviation components.

* Present Affiliation: Skidaway Institute of Oceanography, Savannah, GA 31416.

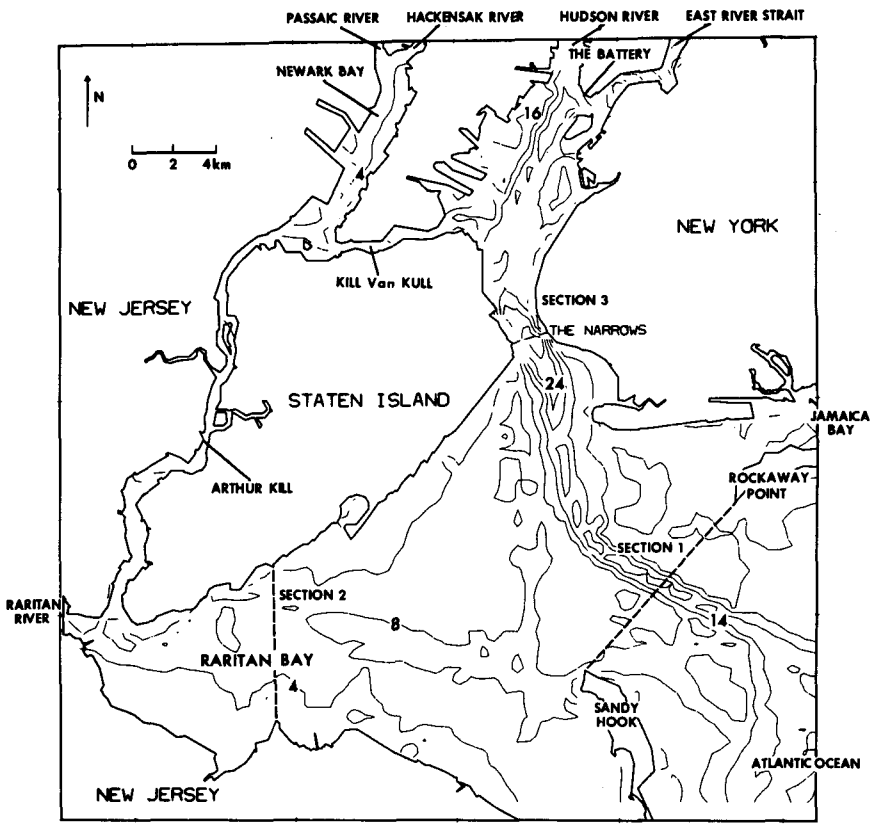

FIG. 1. The locator map and the computational model region of the Hudson–Raritan estuary. Depth contours are in meters below the mean tide level. The three transects where salt and volume fluxes are analyzed are shown.

Consider the normal velocity $u_n(y, z, t)$ at a particular cross section. The horizontal coordinate in the plane of the cross section is y, and z the vertical coordinate. We wish to decompose $u_n(y, z, t)$ into various averages and therefore define

$$(\bar{\cdot})^y = \int_0^Y (\cdot)dy/Y(z)$$

$$(\bar{\cdot})^z = \int_{-H}^0 (\cdot)dz/H(y)$$

where Y is the width at some depth z, and h is the depth at some lateral position y.

As a first step we decompose u_n into a time-averaged term, a spatially independent term, a temporally independent term and the remainder; thus

$$u_n(y, z, t) = [u_0 + u_1(t)] + u_s(y, z) + u_p(y, z, t) \quad (2)$$

where we define

$$u_0 = \langle \overline{\overline{u_n}}^{y,z} \rangle$$

$$u_1(t) = \overline{\overline{u_n - u_0}}^{y,z}$$

$$u_s(y, z) = \langle u_n - u_1 - u_0 \rangle.$$

Note that $\langle u_1 \rangle = \bar{\bar{u}}_s^{y,z} = \bar{\bar{u}}_p^{y,z} = \langle u_p \rangle = 0$.

For the second step we further decompose u_s and u_p such that (see Fig. 2)

$$u_s(y, z) = u_{st}(y) + u_{sv}(y, z)$$

$$u_p(y, z, t) = u_{pt}(y, t) + u_{pv}(y, z, t) \quad (3)$$

where we define

$$u_{st}(y) = \overline{u_s}^z$$

$$u_{pt}(y, t) = \overline{u_p}^z.$$

Note that $\overline{u_{sv}}^z = \overline{u_{pv}}^z = 0$. In order to satisfy previous constraints on u_s and u_p we require that $\overline{u_{st}}^y = \overline{u_{pt}}^y = \langle u_{pt} \rangle = \langle u_{pv} \rangle = 0$. The complete decomposition is then

$$u_n(y, z, t) = u_0 + u_1(t) + u_{st}(y) + u_{sv}(y, z) + u_{pt}(y, t) + u_{pv}(y, z, t). \quad (4a)$$

Similarly, we decompose $S(y, z, t)$ so that

$$S(y, z, t) = S_0 + S_1 + S_{st} + S_{sv} + S_{pt} + S_{pv}. \quad (4b)$$

We now substitute (4) into (1), define the cross-sectional area $A(t)$ as a sum of its time-averaged value A_0 and a deviation $A_1(t)$ and obtain

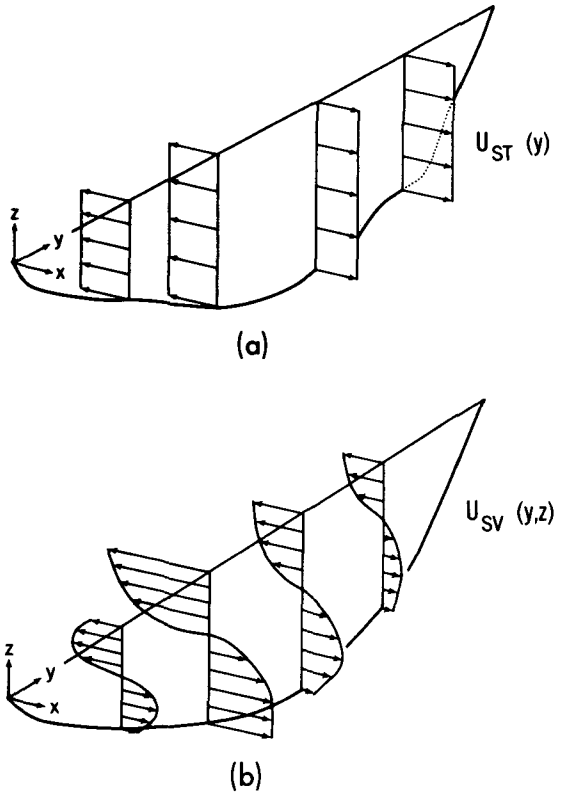

FIG. 2. Decomposition of the cross-sectional deviation of velocity into a transverse deviation $u_{st}(y) + u_{pt}(y, t)$ and a vertical deviation $u_{sv}(y, z) + u_{pv}(y, z, t)$. Shown in this figure are u_{st} and u_{sv} but similar sketches are applicable at a fixed time for u_{pt} and u_{pv}.

important. The third and fourth terms are generally small. The first two terms in (6) are steady, shear dispersion terms due to circulation induced by bathymetry, horizontal density gradients and steady wind effect. The last two terms in (6) are unsteady shear dispersion terms due to tidal (oscillatory) shear and unsteady wind effects.

b. *Problems in determining the averaging period* T

To calculate the "equilibrium" salt flux terms in (5) we must use a large enough averaging period T to "filter out" influences produced by subtidal forcings by spring–neap tidal cycle and winds, for example. Evidence of subtidal forcing by winds can be seen in Fig. 3, which shows a low-pass filtered series of simulated (observed values at Sandy Hook give almost identical results), sectional width-averaged elevation [A_1/(section width)] at the SHRP transect and of east–west component wind stress τ_{0x}. Visual correlation between the wind and sea level can be seen from this figure; a westward (eastward) wind causes sea level to rise (fall). More detailed spectral analyses give good spectral correlation between sea levels and winds at periods of 3 days, and 8–16 days. There are also significant correlations at periods of about 4 days and 10–20 days between sea level and the wind stress that makes an angle of about 50° clockwise from true north direction (approximately parallel to the alongshore direction in the continental shelf region). Thus a significant amount of sea level variation (hence volume and salt transports) in the es-

$$\dot{M} = (u_0A_0 + \langle u_1A_1\rangle)S_0 + A_0\langle u_1S_1\rangle + u_0\langle A_1S_1\rangle + \langle A_1u_1S_1\rangle + \left\langle \int_A u_2S_2 dA \right\rangle \quad (5)$$

where

$$\left\langle \int_A u_2S_2dA \right\rangle \approx \int_A u_{st}S_{st}dA_0 + \int_A u_{sv}S_{sv}dA_0 + \left\langle \int_A u_{pt}S_{pt}dA_0 \right\rangle + \left\langle \int_A u_{pv}S_{pv}dA_0 \right\rangle \quad (6)$$

in which the triple correlation terms involving A_1 have been neglected in (6). In order to assess the magnitude of the triple correlation we have nevertheless retained $\langle A_1u_1S_1\rangle$ in (5) and we shall see that this term is generally smaller than the other terms. The first term in (5) is $(u_0A_0 + \langle u_1A_1\rangle)S_0 = Q_fS_0$ and is the net seaward advection by freshwater discharge, Q_f. The second term accounts for "trapping" effects due either to coastline irregularities and/or bottom topography variations. Fischer (1972) neglected this term in his salt flux analysis of the Mersey Narrows. He pointed out in a later paper (Fischer, 1976) that it could be

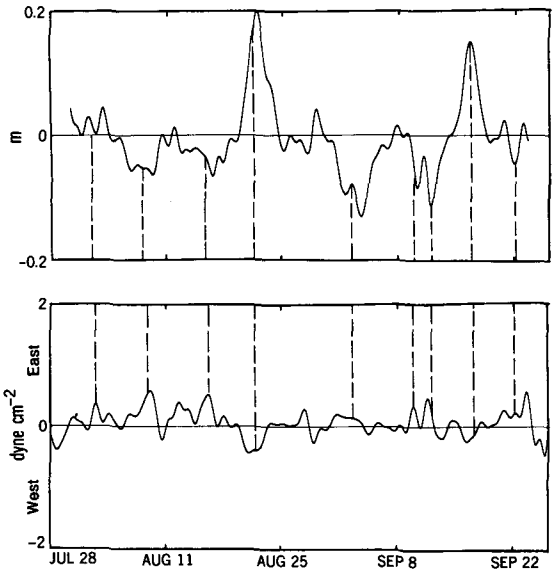

FIG. 3. Low-pass filtered plots of the temporal deviation of sectional width-averaged elevation (m, top panel) at the Sandy Hook–Rockaway Point transect and the east–west component wind stress (dyn cm^{-2}, bottom panel), both for a time period from 28 July through 26 September 1980. Vertical dashed lines denote times when sea levels and winds are visually correlated.

tuary is forced by large-scale winds over the adjacent shelf areas.

Combination of tidal constituents M_2, S_2 and N_2 also produces long-period oscillations. Figure 4a gives low-pass filtered values of u_1A_1 for the three selected cross sections from 28 July through 26 September 1980, and shows variations in Stokes transports in response to spring–neap tidal cycles. A minimum averaging time appears to be 30 days (see Appendix). If short-period records are used the results may therfore be misleading. Figure 4b gives a 6-day running average of volume transport $\int u_n dA$ across the SHRP transect and shows abnormally large outflows (positive) during neap cycles and inflows during spring cycles (similar results are also obtained for the salt flux $\int u_n S dA$). These results illustrate the difficulty of deciding on a particular averaging period to define equilibrium fluxes in an estuary. We shall therefore look at the asymptotic behavior of various fluxes as T becomes large.

3. Mechanisms for salt transport

We list in Table 1 correlation terms that appear on the right-hand sides of Eqs. (5) and (6). Figure 5 gives an example of variations of term (a)–(f) for the SHRP transect as functions of the averaging time T. Similar plots are also obtained for the Raritan Bay and the Narrows sections. In general, we need at least 30 days of data to define meaningful "steady" salt fluxes. In the Raritan Bay section, where the depth is shallow and tidal currents are relatively weak, effects of winds are more significant (in Fig. 4a, midpanel, short-period oscillations are apparent). As a result, we found greater subtidal variabilities in Raritan Bay and an averaging time of about 50 days was required for equilibrium. Thus, an estuary is a slowly varying dynamical system and a long observational record is needed to quantify the different processes (Elliott, 1978).

As an example of what controls the physics of subtidal variabilities in the individual salt flux term, we show in Fig. 6 six-day running averages of terms (d) and (f) in the SHRP transect (solid lines) and in the Narrows section (dashed lines). Term (d) in both cross sections is largest during neap tides (around 17 August and 17 September), caused by generally smaller mixing, and therefore larger vertical deviations in velocity and salinity. This effect of vertical mixing on vertical profiles of velocity and salinity can also be deduced from Hansen and Rattray's (1965) theoretical model. Vertical mixing has similar effects on term (f) except that the magnitude of this term decreases when the ratio R_T of the tidal period T_0 to the time scale T_c for vertical mixing decreases (Holley *et al.*, 1970). The decrease is pronounced when R_T drops below a value of about 0.4. Since $T_c \sim H^2/K_H$, where H is the depth and K_H is the vertical turbulent diffusivity for salt, smaller K_H may actually lead to a decrease in term (f), and this decrease is more pronounced in deeper regions of the

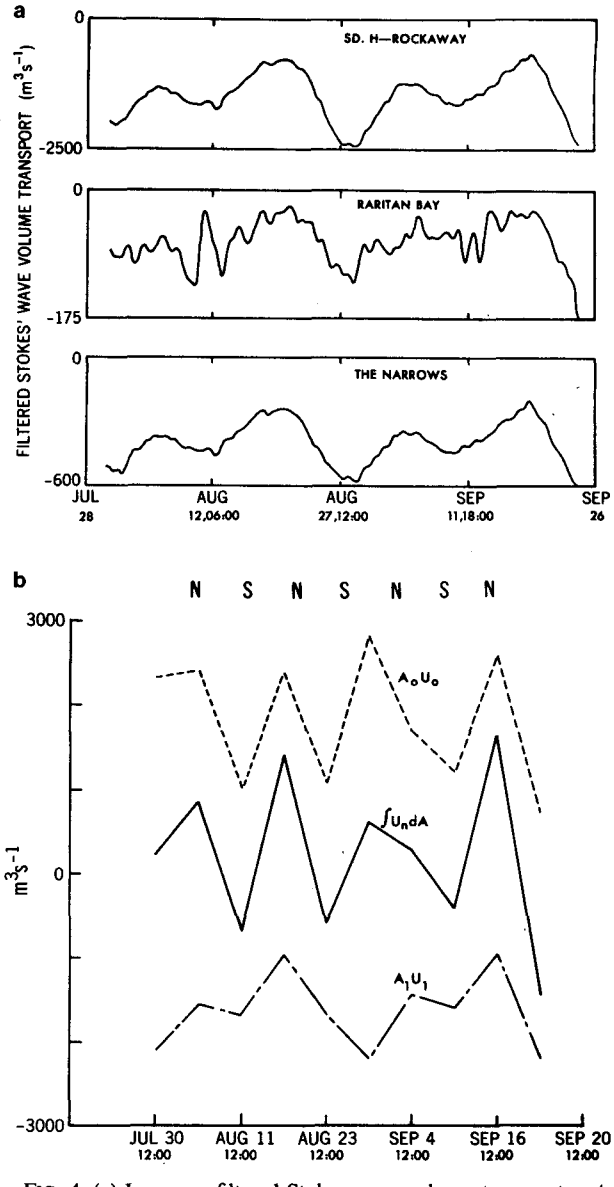

FIG. 4. (a) Low-pass filtered Stokes wave volume transport u_1A_1 ($m^3\ s^{-1}$) at the Sandy Hook–Rockaway Point transect (top panel), the Raritan Bay section (middle panel) and the Narrows section (bottom panel) during the period from 28 July through 26 September 1980. (b) Six-day running average of the Stokes wave volume transport u_1A_1 and volume outflux $\int u_n dA$ across the Sandy Hook–Rockaway Point transect. The "Eulerian" transport A_0u_0 is obtained by adding $\int u_n dA$ to the absolute value of u_1A_1. The approximate neap (N) and spring (S) periods are indicated on the top of the plot.

estuary. We estimated that during neap tides $R_T \approx 1$ at SHRP transect ($H \approx 10$ m, $K_H \approx 25 \times 10^{-4}$ m^2 s^{-1}) and $R_T \approx 0.3$ at the Narrows section ($H \approx 20$ m, $K_H \approx 25 \times 10^{-4}$ m^2 s^{-1}). Thus R_T has little effect on term (f) at the SHRP transect and the behavior with time of term (f) is similar to that of term (d) (Fig. 6, solid line). At the Narrows section the theory of Holley *et al.* (1970) predicts reductions of term (f) during neap tides. This appears to be the case as can be seen from

TABLE 1. Correlation terms for Eqs. (5) and (6).

Term	Expression	Definition	Physical processes
(a)	$S_0 u_0 A_0$	Steady discharge	Total discharge
(b)	$S_0\langle u_1 A_1\rangle$	Stokes wave transport (tidal pumping)	
(c)	$A_0\langle u_1 S_1\rangle$	Tidal correlation	Topographic and bathymetric trapping
(d)	$\int_{A_0} u_{sv} S_{sv} dA$	Steady shear dispersion	Gravitational circulation, steady wind
(e)	$\int_{A_0} u_{st} S_{st} dA$		
(f)	$\langle \int_{A_0} u_{pv} S_{pv} dA\rangle$	Unsteady shear dispersion	Tidal shear, unsteady wind
(g)	$\langle \int_{A_0} u_{pt} S_{pt} dA\rangle$		
(h)	$\langle A_1 u_1 S_1\rangle$	Triple tidal correlation	Tidal pumping and trapping

the two minima in Fig. 6 during neap tides for term (f) (dashed line).

Table 2 gives the volume flux balance in the region bounded by the three transects plus the transect at entrance to Jamaica Bay. Table 3 gives a summary of the "equilibrium" salt flux components obtained from Fig. 5 (and similar plots for the Narrows and the Raritan Bay sections) and shows the relative importance of various salt transport mechanisms in the estuary. The sum of triple correlation terms, except for (h), are obtained from subtracting the sum of terms (a)–(h) from $\dot{M}$, and are less than 10% of (a) plus (b). From NOS observations at the SHRP transect and at the Narrows section we were able to estimate some of the terms in the salt balance equation and these estimates are also given in Table 3. The last row of Table 3 is Hunkin's (1981) 25-hour observations at the Narrows.

Table 2 also includes the model's estimates of equivalent one-dimensional salt dispersion coefficients

$$K = -[\text{sum of terms (c) through (h)}]/A_0(dS_0/dx).$$

These are dispersion coefficients one would use if the estuary were treated as one-dimensional and one were interested in the extent of salinity intrusion in the estuary. Values of K in the Narrows section and in the SHRP transect are large (≈ 500 m^2 s^{-1}) and are of the order found in other estuaries. (In the Mersey Narrows of England, for example, $K \approx 360$ m^2 s^{-1}; Fischer, 1972). In Raritan Bay $K \approx 50$ m^2 s^{-1} so that K increases seaward at a rather rapid rate.

a. *Description of salt flux terms and comparison with observation*

In the following, we shall summarize and compare, whenever possible, simulated and observed salt flux terms listed in Tables 1 and 3. For a summary of the NOS observational program and locations of moored current and conductivity meters, the reader is referred to Part II.

1) TIDAL TRAPPING TERM (c)

Figure 7 gives examples of variations of u_1 and S_1 at the SHRP transect and shows phase shifts of less than $\pi/2$ (with u_1 curves flipped over in the figure) between the two series. Interactive mixing of transect waters with waters from adjacent Sandy Hook Bay and

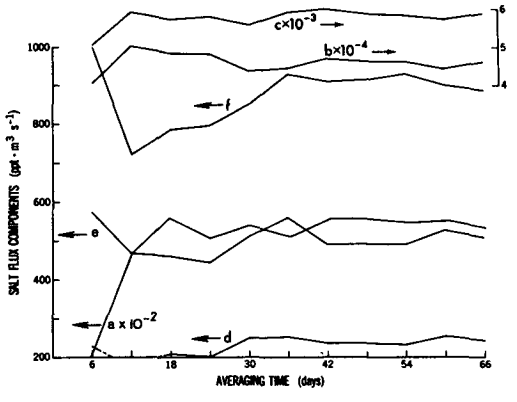

FIG. 5. The "steady" (Eulerian) discharge term "a" and the up-estuary salt flux component terms "b" through "f" (Table 1) as functions of the averaging time for the Sandy Hook–Rockaway Point transect. Term "g" is small and is omitted here.

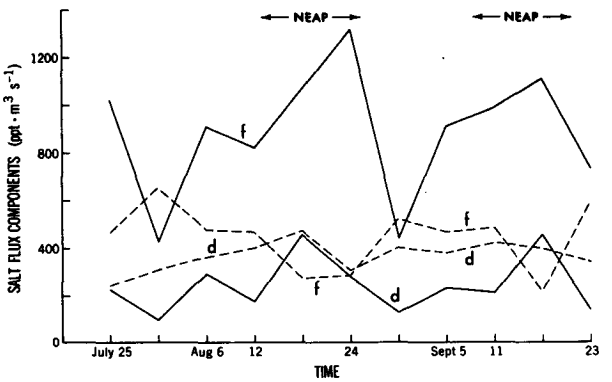

FIG. 6. Six-day running averages of up-estuary salt flux component terms (d) and (f) (Table 1) at the Sandy Hook–Rockaway Point transect (solid lines) and at the Narrows section (dashed lines).

TABLE 2. Computed volume flow through the three analyzed transects plus flow out of Jamaica Bay.* Also included is the 1-D dispersion coefficient, K, which uses information from Table 3 as described in the text.

	A_0 (10^4 m^2)	$\langle Q \rangle = \langle \int u_n dA \rangle$ (m^3 s^{-1})	K (m^2 s^{-1})
Sandy Hook–Rockaway	7.79	180	466
Raritan Bay	3.66	15	50
The Narrows	2.59	161	500
Jamaica Bay		14	

* There is an imbalance of net volume flow of 10 m^3 s^{-1} into the region bounded by the four transects. This imbalance is at least an order of magnitude smaller than subtidal variations in Q (see Fig. 4); one could obtain a zero imbalance by choosing an appropriate end point of the time series for u_n.

Jamaica Bay (see Part I, Fig. 4), which act as "traps" (Okubo, 1973), is responsible for these phase shifts. These phase shifts are more noticeable during neap tides and ebb currents (Fig. 7a), with minimum salinities preceding ends of ebb by as much as one hour. This interactive mixing process is apparently very efficient, and gives rise to a large value of term (c) at the SHRP transect.

Using NOS velocity and salinity measurements at three stations across the SHRP transect (Fig. 1, Part II) we have estimated (25-hour average) values of $u_1 S_1$ by assuming the water to be vertically homogeneous; these are compared in Fig. 8 with the low-pass series of simulated $u_1 S_1$. The comparison is obviously crude and the good agreement is perhaps fortuitous. Both observed and simulated series show large subtidal variations, with absolute values of term (c) generally larger during a spring tide than during a neap. Thus larger amplitudes of u_1 and S_1 apparently more than compensate for the nearly $\pi/2$ phase shifts during a spring tide. Term (c) attains zero and even positive values during a neap phase. Our results clearly demonstrate the fallacy of interpreting mean salt fluxes and dispersion processes in an estuary based on short-period observations.

In the Narrows section, rapid expansions of coastlines north and south of the section appear to act as sufficiently efficient "traps" to produce a large value of term (c). Observations during August 1980 are available at three depths in the midsection, but they are not simultaneous in time. Assuming lateral homogeneity we have computed 25-hour running averages of $u'S'$, where $u' = u_1(t) + u_{pv}(z, t)$ and $S' = S_1 + S_{pv}$, for the near-surface and near-bottom current meters. These correlations again display large subtidal variations, as shown in Fig. 9. These plots give estimates of terms (c) and (f) which we partition in Table 3 according to the ratio of simulated (c) to (f). These estimates are crude, since among other things the integration of observed $u'S'$ over the whole section involves terms like $S_1 u_{pv}$ and $S_{pv} u_1$ which could not be separated and hence integrated to zeroes. Our point here is that term (c) is up-estuary, in agreement with the numerical simulation results but in contrast with the 25-hour observation made by Hunkins (1981), shown also in the last row of Table 3. We feel that Hunkins' survey is too short and represents only a synoptic picture of the salt fluxes in the estuary.

We have also calculated term (c) using NOS observations from 10 to 25 October 1980, at a section 2.7 km due north of the Narrows section shown in Fig. 1. During this period, NOS deployed two near-surface and three near-bottom meters across the section. These give more precise, 25-hour averages of term (c) that range from -1500 to -6000 ppt m^3 s^{-1} with a mean of -3500 ppt m^3 s^{-1} over the 16 day period. These values agree well with the model and NOS August estimates given in Table 3.

TABLE 3. Computed and observed salt flux components (ppt m^3 s^{-1}) in New York Harbor.† Refer to Table 1 for the definitions of the terms, (a) to (h). TCT is the sum of all the triple correlation terms except (h). Underlined numbers are estimates from NOS observations during August 1980.

		1-D Advection		Effective 1-D dispersion							
	S_0	(a)	(a) + (b)	(c)	(d)	(e)	(f)	(g)	(h)	TCT	$\langle \int_A u_n S dA \rangle$
Sandy Hook–Rockaway	30.64	52500	6500	−5800 −6000	−240	−508 −2650	−886	−44 −2360	80	611	−287
Raritan Bay	28.13	2452	320	−25	−66	−111	−51	−43	2	−1	25
The Narrows	28.32	15800	3600	−2280 −4580	−367	−181	−446 −950	−18	10	−165	153
Hunkins' Narrows I	27.93	12050	6650*	2321	−3112	−904	−445	−352	0		

* Hunkins obtained this value from an assumed freshwater discharge $\langle Q \rangle$ = 238 m^3 s^{-1}.

† There is an imbalance of net salt flux of 465‰ m^3 s^{-1} into the region bounded by the four transects. About 290‰ m^3 s^{-1} of this imbalance is caused by the imbalance in volume flow in Table 2 (see footnote). The remaining imbalance (175‰ m^3 s^{-1}) results, during this drought period, in a basin salinity difference of 0.43‰ at the end points of the time series.

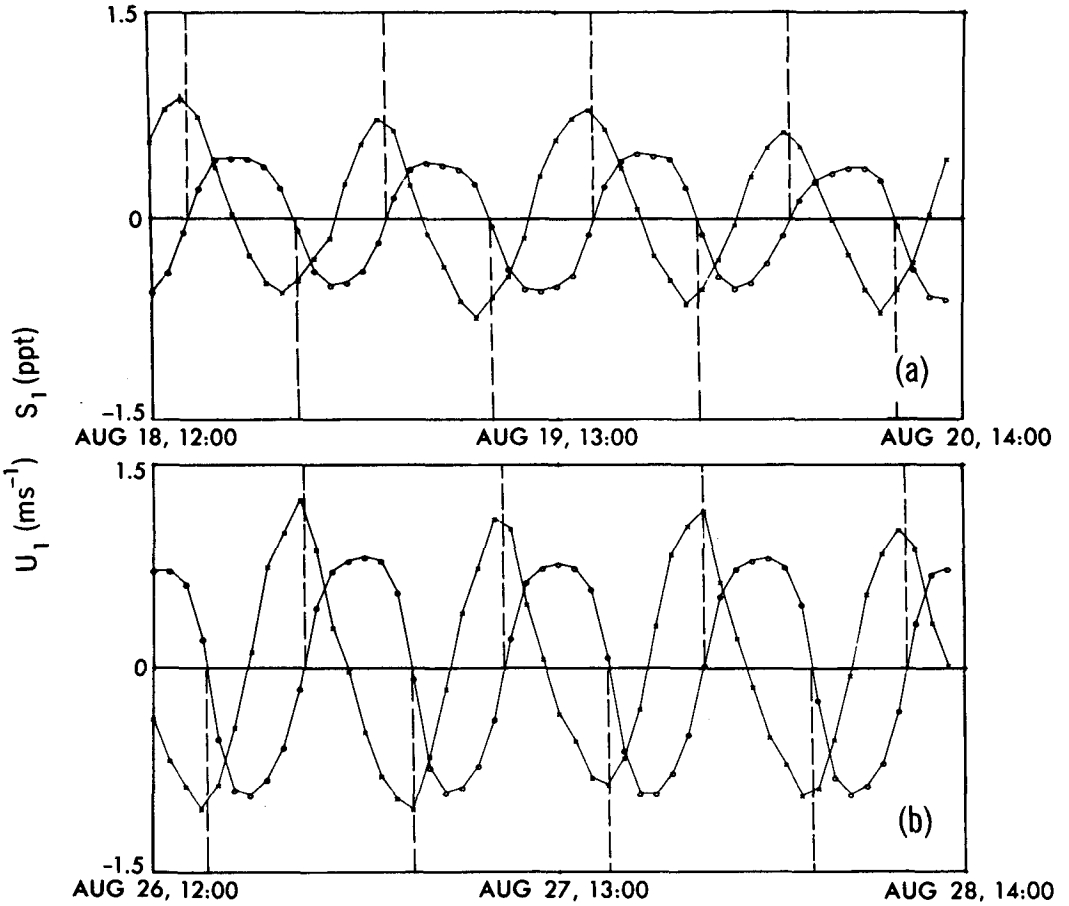

FIG. 7. Time series of u_1 (symbol O, $+ve$ ebbing) and S_1 (symbol ×) at the Sandy Hook–Rockaway Point transect during (a) 1200 EST 18 August through 1300 EST 20 August (neap tide) and (b) 1200 EST 26 August through 1300 EST 28 August (spring tide). Vertical dashed lines denote times of slack waters. (EST = GMT − 5 h)

In Raritan Bay, $\langle u_1 S_1 \rangle$ is small because the tidal currents are weak and the coastline is relatively smooth.

2) OTHER SALT FLUX TERMS

Other salt flux terms display large subtidal variations similar to that for term (c). When short records of less than 50 hours were used in calculating these fluxes we found mean deviations (from equilibrium values) of about ±50% for terms (c) and (f), ±20% for terms (d) and (e) and ±200% for term (g). Spectral analyses suggest that the large variabilities for terms (f) and (g) are related to subtidal wind forcing at 1–2-day and 4–6-day periods. The coherence is especially significant in shallow Raritan Bay where tidal currents are weak.

In Raritan Bay, all up-estuary salt transport terms, except term (c), are important. The steady transverse deviation term (e) is largest and is due to density and wind-induced residual velocities and salinities caused by across-bay bottom variation (Fischer, 1972). However, the sum of vertical deviation terms (d) and (f) is significant and accounts for 40% of total up-estuary salt transport, even though the bay is weakly stratified with surface-to-bottom salinity differences seldom exceeding 0.5‰. This occurs because the bay's coastline is relatively smooth and no large-scale mixing is produced by horizontal eddies. As a result, vertical velocity and salinity deviations are fairly uniform across the bay and their cross-sectional integrals are relatively large.

Estimates of terms (e), (f) and (g) from NOS observations all show larger (in absolute magnitudes) values than simulated values. Apart from the apparent crudeness of these estimates, observations show salt flux imbalances due to the relatively short records (20 days) used. For example, the estimated sum of the three observed up-estuary salt transports (c) + (e) + (g) at the SHRP transect is 1.7 times larger in absolute value than the total seaward salt transport by river discharge.

b. Comparison with Hunkins' results

Hunkins' (1981) estimated fluxes based on his 25-hour (11–12 August 1977) survey at the Narrows section are reproduced here in the last row of Table 3 for comparison with the model and NOS results. Except

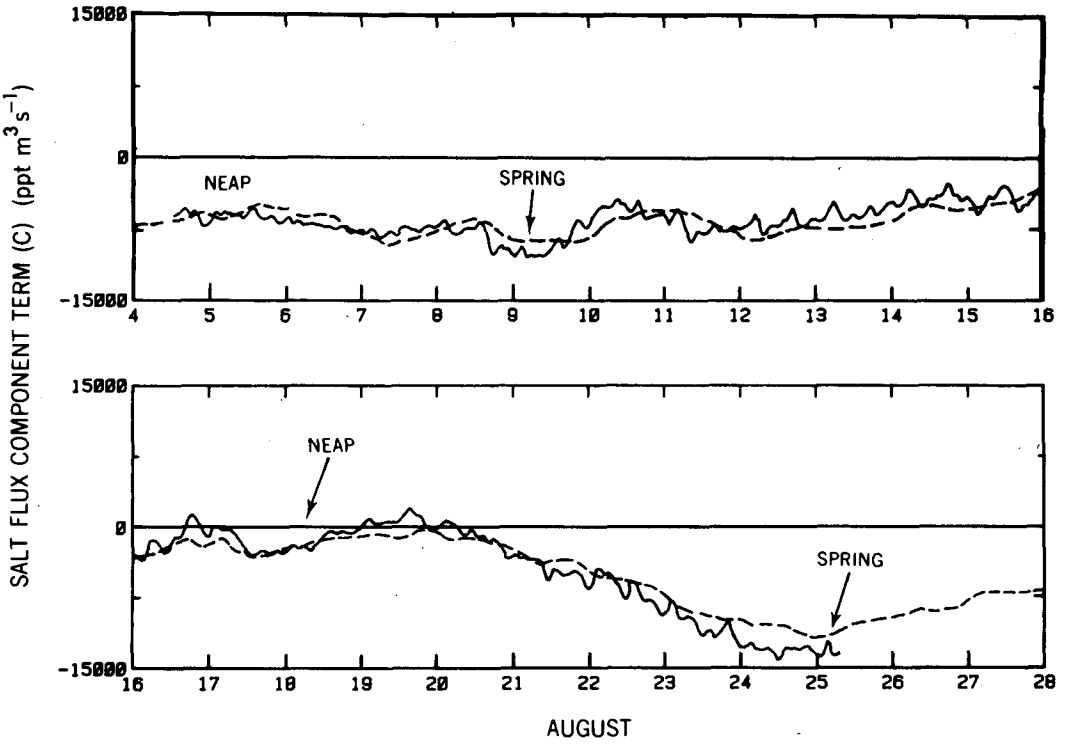

FIG. 8. Low-pass filtered plots of the "trapping" term (c): u_1S_1 calculated from NOS observation (solid lines) and from model results (dashed lines) in the Sandy Hook–Rockaway Point transect.

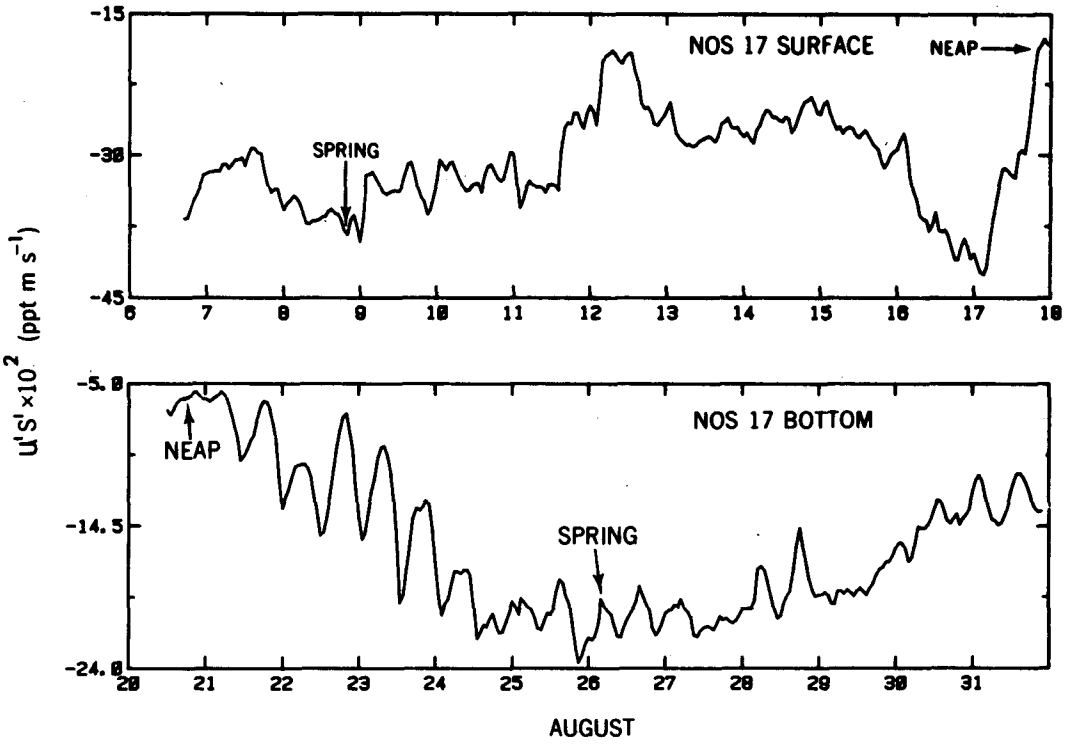

FIG. 9. Filtered (25-h average) plots of the salt flux term (c) + (f): $u'S'$ calculated from NOS observation in the Narrows for near-surface meter (top panel) and near-bottom meter (bottom panel).

for term (f), all other salt flux terms (b), (c), (d), (e) and (g) disagree in magnitude and even in sign [term (c)]. The discrepancy is too large to be explained by the different Hudson River discharges during the two periods (Hunkins' discharge divided by our discharge ≈ 2) and is most likely caused by the subtidal variations we discussed previously. Hunkins attributed the large imbalance, $\dot{M} = 4158$ kg s^{-1}, to subtidal, large-scale wind gradients over the estuary and adjacent shelf areas. This imbalance is an order of magnitude larger than our simulated value of 153 kg s^{-1}.

4. Conclusions

We used two months of model simulation results to analyse salt flux transports in the Hudson–Raritan estuary. These computed fluxes were compared with estimates of fluxes analyzed from 20-day NOS observations. While the sparseness of observational data does not allow exact comparison, observations appear to substantiate model results. The main conclusions are:

1) Unsteady winds and neap–spring tidal variations significantly affect transports of water and salt in the estuary. Salt flux components across a section show large subtidal variations, and long records of data of at least 30 days are required to define a statistically stationary estuary. Analyses of salt dispersion processes based on short time series are not reliable bases for interpretation.

2) Subtidal responses appear to be strongly influenced by forcings from the adjacent continental shelf and our present model, even though forced by real sea level variations at the open boundaries may be an inadequate representation of the reality. Future estuarine modeling should be directed toward an estuary–continental shelf coupled model.

3) In regions of the estuary where there are significant coastline irregularities, cross-sectionally averaged velocity and salinity are out of phase by phase angles that are less than $\pi/2$. This phase angle difference is closer to $\pi/2$ during the flood than it is during the ebb, implying larger upstream salt transport during the ebb. This is called a "trapping" mechanism by Fischer (1976) and is dominant in the SHRP transect and in the Narrows section.

4) Large coastline irregularities produce large, intense horizontal eddies. These eddies reduce the correlation $u_{sv}S_{sv}$ near the coastline and the upstream salt flux induced by the steady vertical deviation term is therefore small. In Raritan Bay, where the coastline is relatively smooth and tidal currents are weak, vertical contributions to up-estuary salt transport are as important as the transverse contributions. This happens despite the fact that surface-to-bottom salinity differences are small (<0.5‰). Moreover, the vertical, unsteady oscillatory shear correlation $u_{pv}S_{pv}$ is important and is a function of unsteady wind forcing and therefore rather difficult to model empirically. In this case, one cannot apply a two-dimensional (xy–t) model to the estuary and hope to obtain realistic results.

Acknowledgments. We wish to thank Susan Salyer for preparing the manuscript. Drs. A. Blumberg and K. Bryan read the first draft of the manuscript and gave many valuable comments. The figures were drafted by P. Tunison and processed by J. Conner. Anna Boyette and Suzanne McIntosh prepared the final version of the figures. This research was sponsored by the New Jersey Sea Grant Program under a grant from the Office of Sea Grant of NOAA, Grant 81 AA-D-0065, Project R/E-3. Additional funding was provided under Grant NA 80 RAD 00033 from the Northeast Office of the Office of Marine Pollution Assessment of NOAA. LYO was supported in part by the Visiting Scientist Program of Princeton University/NOAA, Grant 04-7-022-44017.

APPENDIX

Averaging Period for Equilibrium Flux Calculations

The M_2 and S_2 tidal constituents combine to introduce into u_1A_1 a slow spring–neap amplitude modulation of period 15 days. Thus, even in the absence of time-dependent winds, freshwater discharges and other subtidal forcings, statistics can only be reasonably stationary if the averaging period is about 15 days. We can see this more clearly by considering a straight rectangular channel of length L, where

$$\eta(L, t) = \sum_{n=1}^{N} \eta_n \cos(\omega_n t - \phi_n) \qquad \text{(A1)}$$

at the seaward boundary $x = L$ and $U = 0$ at $x = 0$. In (A1), η_n, ω_n and ϕ_n are the amplitude, frequency and the phase, respectively, of the nth tidal constituent. The solution at any point x can also be Fourier decomposed and written in the form (A1), but with η_n and ϕ_n functions of x.

From continuity equation with $V = 0$ we obtain

$$\eta_t + \left(\int_{-H}^{0} U dz\right)_x + (U_{z=0}\eta)_x + O(\eta^2) = 0,$$

which we can integrate with respect to x from $x = 0$ to $x = L$ and obtain, after neglecting the $O(\eta^2)$ terms

$$\int_0^L \eta_t dx = -\int_{-H}^{0} U dz - U|_{z=0} \cdot \eta.$$

We can now time average this last equation and obtain

$$T^{-1} \int_0^L [\eta(x, T) - \eta(x, 0)]dx = -\int_{-H}^{0} \langle U \rangle dz - \langle U|_{z=0}\eta \rangle. \qquad \text{(A2)}$$

The first term on the rhs of (A2) is the mean Eulerian transport and the second term is the mean Stokes

transport (Longuet-Higgins, 1969), both at $x = L$. Their sum is therefore the mean Lagrangian transport at $x = L$. If the estuary is in a steady state with zero freshwater inflows, both $\langle$Lagrangian transport$\rangle$ and the $d/dt(\langle$Lagrangian transport$\rangle)$ must be zero. From (A1) and (A2) we see that the averaging period T, for which this mean is defined, depends on η. For example, if $N = 2$, $\omega_1 > \omega_2$ where ω_1 is the S_2 frequency and ω_2 is the M_2 frequency, and if also $\phi_1 = \phi_2 = 0$ and $\eta_1 = \eta_2 = 1$, we have, at a particular x

$$\eta(x, t) = 2^{1/2}(1 + \cos\Delta\omega t)^{1/2} \cos(\omega_2 t - \Phi)$$

where

$$\Phi(t) = -\tan^{-1}[\sin\Delta\omega t/(1 + \cos\Delta\omega t)], \quad \Delta\omega = \omega_1 - \omega_2.$$

It can now be shown that if a short record of a few tidal cycles mT_2, $T_2 = 2\pi/\omega_2$, $m < 6$ say, is taken, the magnitude of the unsteady term

$$\eta(x, mT_2) - \eta(x, 0) \approx 0.75(\Delta\omega m T_2)^2 + \cdots \approx 4 \times 10^{-2}, \quad \text{for} \quad m = 1.$$

This can be compared with the unsteady term for which a longer record of 15 days (i.e., the long record is taken to be close to $2\pi/\Delta\omega$, the spring–neap tide period) is used:

$$\eta(x, T) - \eta(x, 0) \approx 0.75(\Delta\omega\Delta p)^2 + \cdots \approx 3 \times 10^{-4},$$

where $\Delta p = 15 \text{ days} - 2\pi/\Delta\omega \ll 1$.

REFERENCES

Elliott, A. J., 1978: Observations of meteorologically induced circulation in the Potomac estuary. *Estuarine Coastal Mar. Sci.*, **6,** 285–299.

Fischer, H. B., 1972: Mass transport mechanisms in partially stratified estuaries. *J. Fluid Mech.*, **53,** 671–687.

——, 1976: Mixing and dispersion in estuaries. *Annual Review of Fluid Mechanics,* Vol. 8, Annual Reviews, 107–133.

Hansen, D. V., and M. Rattray, 1965: Gravitational circulation in straits and estuaries. *J. Mar. Res.*, **23,** 104–122.

Holley, E. R., D. R. F. Harleman and H. B. Fischer, 1970: Dispersion in homogeneous estuary flow. *J. Hydraul. Div. Proc. ASCE,* **96,** 1691–1709.

Hunkins, K., 1981: Salt dispersion in the Hudson estuary. *J. Phys. Oceanogr.*, **11,** 729–738.

Longuet-Higgins, M. S., 1969: On the transport of mass by time-varying ocean currents. *Deep-Sea Res.*, **16,** 431–447.

Oey, L.-Y., G. L. Mellor and R. I. Hires, 1985a: A three-dimensional simulation of the Hudson–Raritan estuary. Part I: Description of the model and model simulations. *J. Phys. Oceanogr.*, **65,** 1676–1692.

——, G. L. Mellor and R. I. Hires, 1985b: A three-dimensional simulation of the Hudson-Raritan estuary. Part II: Comparison with observation. *J. Phys. Oceanogr.*, **15,** 1693–1709.

Okubo, A., 1973: Effects of shoreline irregularities on streamwise dispersion in estuaries and other embayments. *Neth. J. Sea Res.*, **6,** 213–224.